

# Stabilization study at the sub-nanometer level at the interaction point of the future Compact Linear Collider

G. Balik<sup>1\*</sup>, A. Badel<sup>2</sup>, B. Bolzon<sup>1</sup>, L. Brunetti<sup>1</sup>, B. Caron<sup>2</sup>, G. Deleglise<sup>1</sup>, A. Jeremie<sup>1</sup>, R. Le breton<sup>2</sup>, J. Lottin<sup>2</sup>, L. Pacquet<sup>1</sup>

<sup>1</sup>: LAPP-IN2P3-CNRS - Université de Savoie - Annecy-le-Vieux France

<sup>2</sup>: SYMME-Polytech Annecy Chambéry - Université de Savoie - Annecy-le-Vieux France

\*: gael.balik@lapp.in2p3.fr

**Abstract-** The Compact Linear Collider (CLIC) is currently under design at CERN (European Organization for Nuclear Research). It would create high-energy particle collisions between electrons and positrons, and provide a tool for scientists to address many of the most compelling questions about the fundamental nature of matter, energy, space and time. In order to achieve the required luminosity of  $10^{34} \text{ cm}^{-2}\text{s}^{-1}$ , two beams are accelerated and steered into collision. Considering the desired size of the beams (nanometer scale), the collision will require a very low vertical motion of these two beams all along the collider, and more specially through the last two focusing magnets. Different methods are usually carried out; slowly varying misalignment can be compensated using beam-based control strategy while faster beam motions require a control of the vertical displacement of the different mechanical elements supporting the magnet. This paper describes the different aspects needed to stabilize the beam at the nanometer scale. First of all, sensors capable of measuring sub-nanometer displacement and performing numerical simulations using ground motion measurements are presented. Then an active-passive isolation is studied using vibration sensors and piezoelectric actuators. Finally, a hybrid adaptive filtering algorithm which takes advantage of feedback and adaptive control has been implemented in the simulation layout.

## I. INTRODUCTION

After the world's largest particle accelerator LHC [1], the next generation of accelerators is being designed. Among them, the Compact Linear Collider CLIC is an ambitious project that proposes colliding beams of positrons and electrons

One of the major challenges is to achieve luminosity that the experiments demand. This can be done only by focusing and colliding the two separate beams to nanometer spot sizes. Thus, it imposes very tight constraints on the final focus (FF) system's alignment and stability.

The future CLIC composed of two arms of approximately 17 km long facing each other will accelerate beams at velocities near the speed of light. Once accelerated with the required energy and emittance [2] through the main linac, a sophisticated beam delivery system focuses the beam down to dimensions of 1 nm RMS size in the vertical plane and 40 nm horizontally. This requires the final focus magnets to be stabilized to a vibration amplitude of less than 0.1 nm for oscillations above 0 Hz at the interaction point (IP). Figure 1 represents a scheme of the compact linear collider at the interaction point.

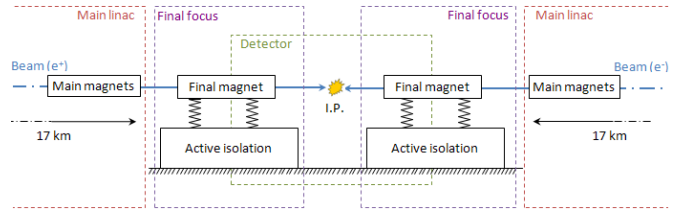


Figure 1. Compact Linear Collider layout at the interaction point.

This paper proposes a method to deal with ground vibrations. A first part aims to establish a comparative table of the sensors needed to measure at the nanometer scale. Then a study of a dedicated active-passive isolation currently under development is presented and compared to a commercial solution. Next, a filtering algorithm combining feedback, adaptive algorithm and active-passive isolation is presented and numerical simulations have been performed. This paper ends up with a robustness study and a global pattern study of the active-passive isolation needed to achieve the requirements.

## II. SENSORS FOR THE SUB-NANOMETER LEVEL

### A. Instrumentation

Beam components like the focusing magnets have to be stabilized to the sub-nanometer level. Thus the sensors have to be reliable for measurements in the same range and they need to have good resolution down to the sub-nanometer level in the frequency range 0.1 Hz to 100 Hz. In addition, since the sensors have to perform in an accelerator environment, they need to be radiation hard and still work in a magnetic field.

When measuring nano-displacements, resolution of the measurement chain is limited by internal noise of the chain itself, mainly composed of sensors and acquisition system noises. Consequently, these noises have been measured and described in [3].

Our approach was to study commercial sensors that could answer the sensor specifications. Table I gives the specifications of the sensors used.

The Güralp sensors are high sensitive electromagnetic geophones measuring velocity in 3 directions (vertical and 2 horizontal). They have a flat frequency response from 0.03 Hz to 50 Hz. However, depending on the site, the internal noise decreases with frequency, so they are useful for our

TABLE I  
TECHNICAL CHARACTERISTICS OF USED SENSORS

Sensor type	Electromagnetic Geophone	Piezoelectric Accelerometer			Electrochimical Geophone	Capacitif
Model	GURALP CMG-40T	ENDEVCO 86	393B12	4507B3	SP500	D-015.00
Company	Geosig	Brüel & Kjaer	PCB Piezotronics	Brüel & Kjaer	EENTEC	Physik Instrumente
Output signal	Velocity (X,Y,Z)	Z acceleration			Velocity	Distance
Sensitivity	1600 V/m/s	10 V/g	10 V/g	98 mV/g	2000 V/m/s	0.67 V/ $\mu$ m
Bandwidth [Hz]	[0.033-50]	[0.01-100]	[0.05-2000]	[0.3-6000]	[0.0167-75]	[0-3000]
Mass [g]	7500	771	210	4.9	750	<10

measurements from 0.1Hz to 50Hz. The Endevco sensors are high sensitive piezoelectric accelerometers measuring in the vertical direction with a flat frequency response between 0.01Hz and 100Hz. However, their internal noise at low frequency combined to the fact that at low frequency, ground acceleration is very low; the useful range is closer to 10 Hz - 100 Hz. Both types of sensors are used for the measurements, the Guralp for the low frequency range and the Endevco for the upper frequency range.

Sensor data was acquired with a PULSE acquisition system with a 16 bits 7537A controller by Brüel&Kjaer [4] combined with amplifiers to increase the dynamic range.

The parameters used for the measurements and the details of the data analysis using the Power Spectrum Density (PSD), the Coherence and the Integrated Root Mean Square (RMS) can be found in [5].

### III. PASSIVE /ACTIVE ISOLATION

In an accelerator environment, many sources of disturbances such as ground motion, pumping devices, acoustic vibrations, cooling systems and others are present, sources which generate vibrations several orders of magnitude larger than the beam size. Stabilization of accelerator components such as the final focus is critical if the desired nanometer beam sizes are to be reached. For this study, the reference ground motion is the one measured in the tunnel of the Large Hadron Collider (LHC) [6] at CERN and more precisely, the ground motion where is located the Compact Muon Solenoid (CMS) calorimeter [7]

Plots 2 and 3 represent the PSD and the integrated RMS displacement of the ground motion measured at LAPP (Annecy) and at the CMS.

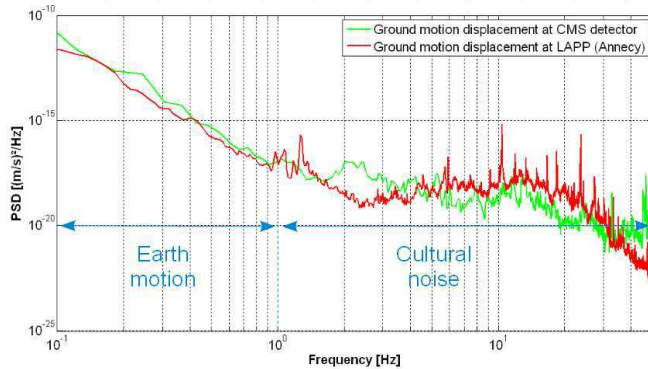


Figure 2. PSD displacement measured at LAPP and CMS site

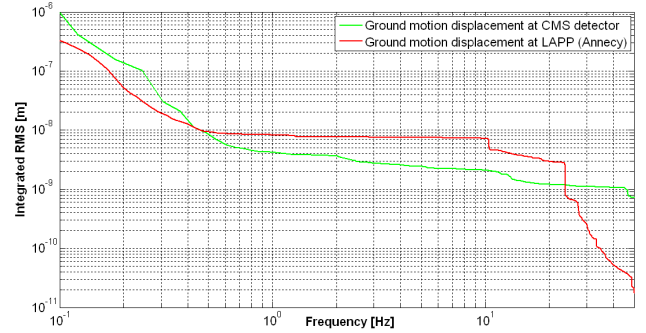


Figure 3. Integrated RMS displacement of ground motion at LAPP and CMS site

Measurements were performed thanks to geophones detailed Table 1.

#### A. ATF2 (Accelerator Test Facility)

A first approach studied in [8] aims to design a single rigid structure supporting both magnets at each side of the IP. It is based on the fact that a good spatial coherence of the ground motion over a few meters resulting in a relative motion of the Final Doublets (FD) small enough to respect the tolerances. However, coherence in the ground motion falls off rapidly with distance. As magnet vibration tolerances are severe [9] and unprecedented for CLIC (12 m length between FD and a vertical displacement of 0.1 nm integrated RMS instead of 7 nm previously) some of them may induce significant IP beam motion, and would then require dedicated stabilization such as active-passive isolation.

#### B. Passive isolation

One of the key points in control-structure design is the passive structural damping, widely used in the industrial field as well [10]. Passive damping techniques provide a simple method to eliminate structural vibrations, allowing a higher bandwidth control resulting in improved control characteristics and lowered required effort. The main advantage of added passive damping in controlled structures is the improved stability and performance robustness characteristics given plant uncertainties. However, given the tight specifications in this study, the passive isolation itself isn't sufficient enough to meet the requirements.

### C. Active isolation

Before designing a dedicated active isolation, a study [11] of the different commercial solutions aimed to select the most efficient one on the market for this type of application. The selected solution is a TMC table with STACIS feet [12], also described in [3], see figure 4:

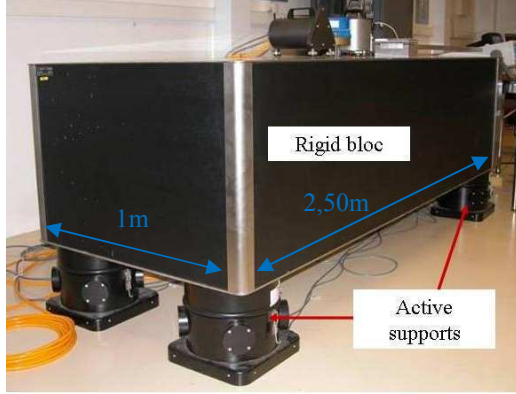


Figure 4. TMC table with STACIS feet

This product is able to manage vibrations at a sub nanometer scale. However it isn't sufficient, and given the tight tolerances, and the cost of such a product, a dedicated solution is being developed. This system is at a prototype stage and could eventually replace the TMC table. As a first approach, its dynamical behavior has been evaluated by a modal analysis that predicts the resonant frequencies of the structure. This finite element model has then been converted into a state space model whose mechanical dynamic effects have been implemented in Matlab/Simulink [13] for further active control study. This active foot (see figure 5) has on the one hand, to be rigid enough to avoid low frequency resonant modes and on the other hand, to let the actuators work.

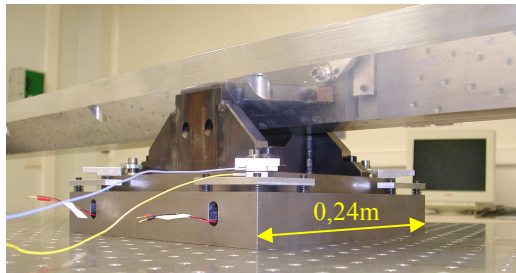


Figure 5. Picture of the active feet under study.

To achieve this compromise, the foreseen supporting system includes deformable parts made of elastomeric material which provide the mechanical guidance and allow the micrometric displacements of piezoelectric actuators. This strategy presents the advantage to avoid sliding mechanisms and consequently friction effects that could affect the linearity of the system. This active foot includes four piezoelectric actuators and four capacitive sensors measuring the relative distance between ground fixed plate and the isolated one (see figure 6). Such a system is potentially suitable to be handled by three degrees of freedom algorithm controlling the vertical motion and the two associated rotations.

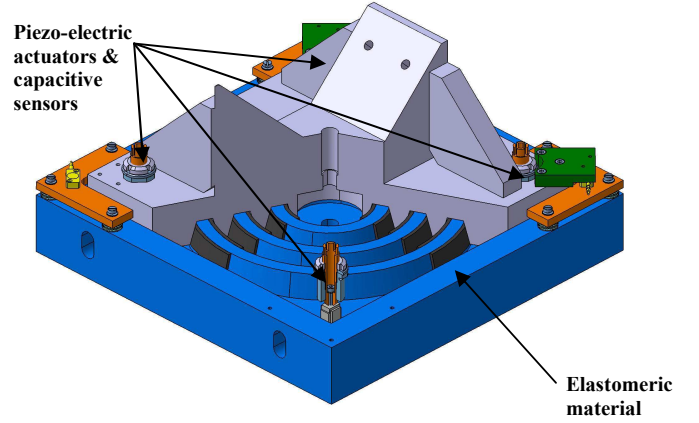


Figure 6. Scheme of the active feet

Piezoelectric actuators used in this active foot have been experimentally tested to check if sub-nanometer motion and measurement was feasible. Thus, two piezoelectric actuators were considered. The first one is a commercial PPA10M from Cedrat® [14] and the second one is a custom one made from a 0.3mm thick piezoelectric PZT patch. Main characteristics of both actuators are summarized in table II. The custom actuator has a much better sensitivity but its maximal displacement is much lower.

TABLE II  
TECHNICAL CHARACTERISTICS OF USED ACTUATORS

	Dimensions	Max Disp	Sensitivity
<b>PPA10M</b>	18x10x6.5mm <sup>3</sup>	8μm	47nm/V
<b>Custom</b>	0.3x10x10mm <sup>3</sup>	85nm	0.5nm/V

Generated displacements were measured using a D-015 sub-nanometer resolution capacitive sensor from Physik Instrumente® (PI) [15] whose theoretical resolution is 0.1nm.

Figure 7 and 8 show the displacement measured on the PPA10M driven by a 20mV – 5Hz sinusoidal voltage and on the custom actuator driven by a 1V – 5 Hz sinusoidal voltage respectively. Signals on the sensor were filtered using a real time 8<sup>th</sup> order Bessel 1kHz low pass filter.

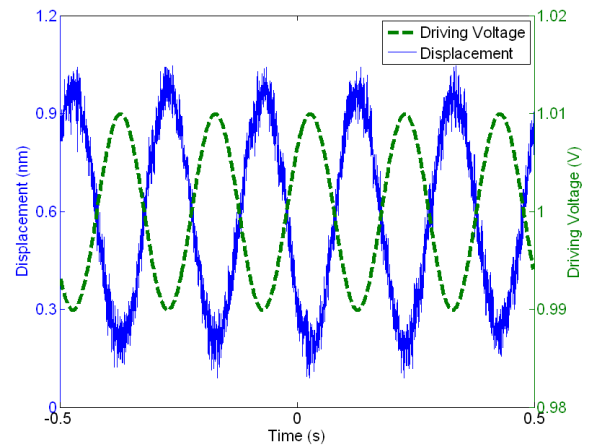


Figure 7. Voltage and displacement for the PPA10M actuator

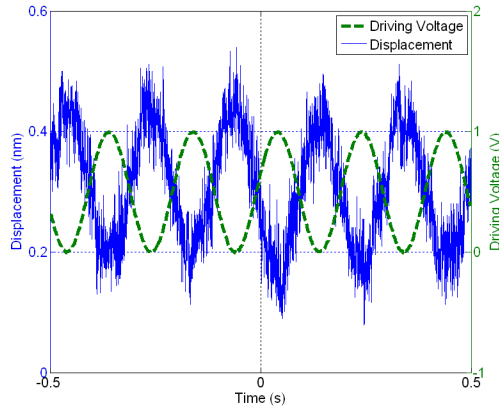


Figure 8. Voltage and displacement for the custom actuator

Measured displacement amplitudes are 0.85nm for the PPA10M and 0.25nm for the custom actuator. In both cases, the noise level is about 0.1nm, which corresponds to the sensor resolution and means that the precision limitation is due to the sensor rather than to the actuators.

The main advantage of the PPA10M actuator is that its displacement range is 100 times larger than the custom one, which means that it could be used for both alignment and stabilization purposes. Its drawback is that sub-nanometer motion requires the driving voltage to be lower than 20mV. Very low driving voltages necessarily induce a deterioration of the voltage signal to noise ratio that could impact the global precision of the motion. A dedicated low noise and large range power supply is then certainly required, as well as high resolution Digital Analog Converters ( $\geq 16$ bits).

#### IV. BEAM TRAJECTORY CONTROL STRATEGY

##### A. Problematic

Once accelerated, the beam goes through a final focusing magnet subject to disturbances (see figure 9). Stabilization of the beam can be obtained by using the corrective capabilities of the beam components by measuring the beam parameters (size, position...) tanks to a Beam Position Monitoring (BPM) (not represented) and acting on the beam with a kicker. This frequency range in which this is possible is given by the beam repetition rate. For CLIC, this rate is 50Hz (which means that the beam is composed of a serial of trains separated from each other in time by 20 ms). This configuration imposes that the beam cannot be corrected above 5-6Hz. As ground motion is still at a detrimental level until about 50-100Hz, depending on the site, it needs to be corrected by mechanical means. Thus, this magnet stands on an active-passive support designed to reduce ground motion vibrations.

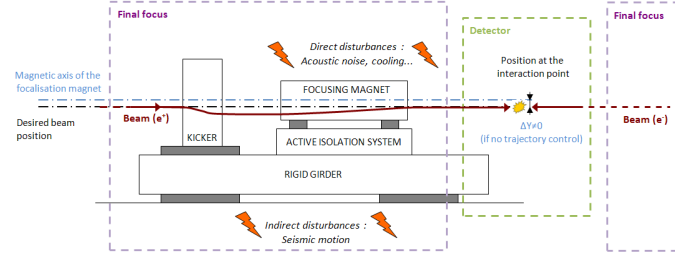


Figure 9. Final focus scheme.

A new generation of beam instrumentation will be required to commission and tune a future linear collider. At this stage of the CLIC construction, most elements of this process are still under development. It was thus necessary to make some assumptions concerning sensor and actuator behavior. First, the BPM used to obtain the beam-beam offset at the IP isn't influenced by the ground motion as it measures a highly amplified image of the relative displacement  $\Delta Y$  (ratio:  $10^5$ ). Next, the kicker designed to provide a corrective kick isn't influenced by the ground motion as well because it generates a uniform magnetic field to steer the beam.

##### B. Control

The proposed control framework is composed of a feedback loop where the controller ( $H$ ) defines the dynamical behavior of the system and a real-time adaptive control feature ( $H_a$ ) based on the Generalized Least Square (GLS) [16] algorithm manages to estimate and cancel out the disturbance. The structure of this control is given in figure 10 (The backward shift operator is denoted  $q^{-1}$ ).

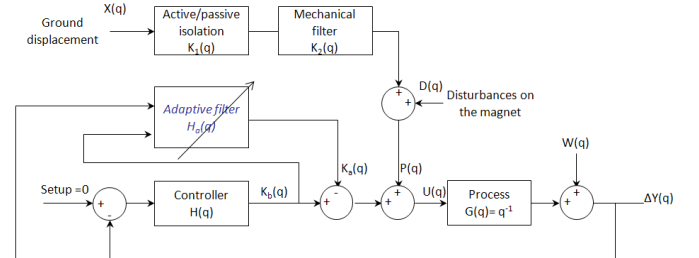


Figure 10. Scheme of the beam trajectory control.

The disturbance ( $X$ ) is the mechanical excitation from ground motion which is represented by the ground motion displacement measured at the Compact Muon Solenoid (CMS) detector [17]. Other sources of disturbance than ground vibrations are neglected as their contribution to the beam motion is supposed to be insignificant compared to the ground motion itself.

One has considered in the simulated layout that the final focus magnet will be placed on an active isolation system (an active table) whose dynamical behavior has been inspired by the TMC table by using several measurements. It has been integrated in the theoretical model ( $K_1$ ). However, this active isolation system isn't efficient enough to decrease sufficiently the integrated RMS displacement at 5-6Hz. The presence of a passive isolation ( $K_2$ ) (such as a flexible mechanical support placed under the magnet) has therefore been added in the



simulation layout. It should behave as a second order low pass filter with a resonant frequency of 2Hz and a damping ratio of 0.01. ( $P$ ) is finally the disturbance felt by the magnet.

The transfer function between the mechanical displacement of this magnet and the beam can be modeled by a constant matrix (equal to 1 in the model), the disturbance on the magnet ( $D$ ) is added to the displacement of the active isolation, the noise of the sensor ( $W$ ) is added to the displacement of the beam.

The action ( $K_b$ ) meant to reduce the motion of the beam (or the offset between the two beams at the interaction point) is done by a kicker. The obtained displacement of the beam is proportional (equal to 1 in the following model) to the injected current of the kicker. The dynamic of the system is due to the frequency of the beam train, so the process can be treated as a first approach as a delay at a sampling period equal to 0.02 s.

This scheme allows to design a controller ( $H$ ) that performs optimally to minimize the integrated RMS displacement of the beam. This optimization has to be done once, before using the process and depends on the PSD of the ground motion.

### C. Numerical simulations

Numerical simulations on a beam structure demonstrate how the proposed control minimizes vibration caused by the ground motion.

The following figures show the obtained performance:

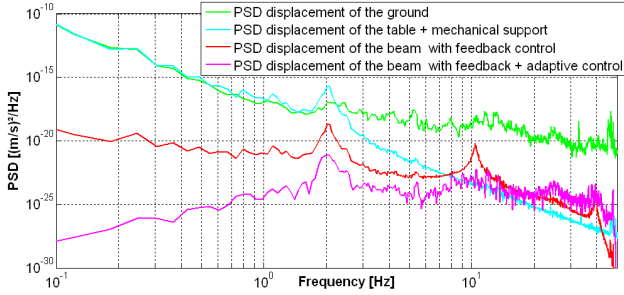


Figure 11. PSD obtained with feedback and adaptive control.

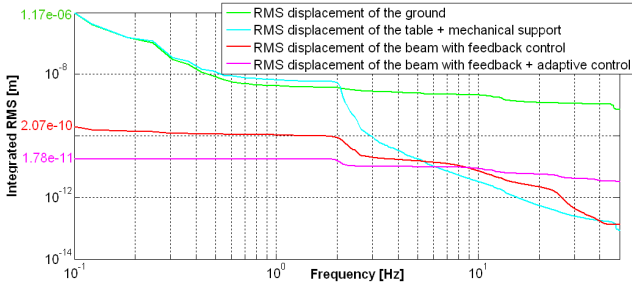


Figure 12. Integrated RMS obtained with feedback and adaptive control.

The simulation shows that this strategy combining active-passive isolation to damp fast motion of the ground and feedback loop coupled with an adaptive algorithm which deals with slower motions is able to reach an integrated RMS at 0.1 Hz of  $1.78e^{-11}$  m.

The previous study is based on a model of the real system currently under development. Considering the current project status, it was thus necessary to make several assumptions and to arbitrarily fix certain parameters. A robustness study is proposed to show the good behavior of this control.

### D. Robustness

Next figure shows the integrated RMS displacement of the beam obtained if the mechanical support isn't correctly characterized (due to model imprecision, or parameters drift).

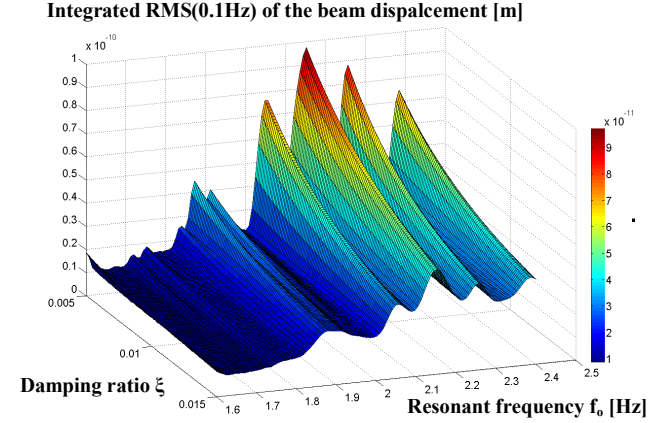


Figure 13. Integrated RMS(0.1Hz) versus mechanical support characteristics.

The parameters  $\xi$  and  $f_0$  from the mechanical support vary respectively from  $\pm 50\%$  and  $\pm 10\%$ . Several waves can be observed representative of the different excitation waves of the process. The worst case where  $\xi=0.005$  and  $f_0=2.2$  Hz implies an integrated RMS(0.1Hz) of about 0.1nm which is at the thresholds of the requirements. This means that the control strategy has a good robustness with respect to unmodelled or neglected dynamics.

It is also necessary to study the influence of the sensor's noise on the control behavior. Figure 14 shows the variation of the integrated RMS displacement of the beam versus the noise of the BPM (represented by a white noise ( $W$ ) added to the measured displacement).

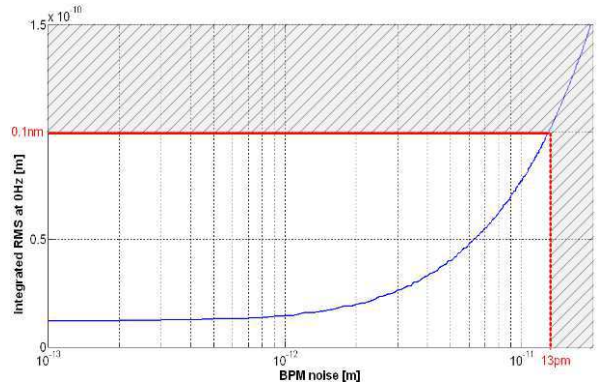


Figure 14. Variation of the integrated RMS displacement at 0 Hz versus BPM noise.

The level of sensor's noise is crucial for a good performance of the control. It cannot exceed 13 pm integrated at 0.1 Hz to respect the specifications.

Considering the amplification ratio of  $10^5$  of the BPM, and the value of the most detrimental integrated RMS displacement of the ground of 1.17  $\mu\text{m}$  (see figure 12), the worst case would imply a noise of 11.7 pm integrated at 0.1 Hz, which is obviously compatible with our previous results.

#### E. Pattern of the desired active-passive isolation dynamic

This part aims to establish a pattern of the global transfer function ( $K_g = K_1 K_2$ ) needed between the ground and the beam to reach the specifications of 0.1 nm. This transfer function should be representative of a typical mechanical support dynamical behavior. Thus, it has been modeled by the following 2<sup>nd</sup> order low-pass filter:

$$K_g(s) = \frac{G_0}{1 + \frac{2\xi}{\omega_0}s + \frac{1}{\omega_0^2}s^2} \quad \text{with } \omega_0 = 2\pi f_0$$

The adopted strategy consisted in replacing  $K_1$  and  $K_2$  in figure 10 by  $K_g$  with variable parameters and to optimize the controller until an eventual solution allows to reach the specifications. The body of the combinations ( $f_0$ ,  $G_0$ ), see figure 15, constitutes the pattern of the desired active-passive isolation dynamic.

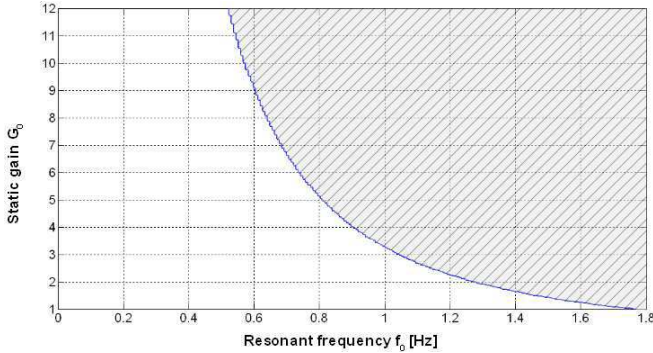


Figure 15. Pattern of the active-passive isolation dynamic.

The area under the curve represents the body of the combinations of ( $f_0$ ,  $G_0$ ). The simulation showed that this pattern is independent of the damping ratio  $\xi$  in the range [0.005 0.7]. This results from the extremely high efficiency of the beam trajectory control in low frequencies.

Such a pattern could be used for a more detailed study of a mechanical support design. This support, if realizable, could be efficient enough to achieve the desired performances.

#### V. CONCLUSION

In this paper we have presented our methodology of the stabilization of the future Compact Linear Collider. The approach can be applied to any similar project. Combining real time control algorithm based on an adaptive scheme and commercial active-passive isolation made it possible to actively reject structure vibrations below 0.1 nm at 0.1 Hz. The

study opens up perspectives for the construction of an active-passive isolation support as well. Thus, a dedicated solution is currently being designed thanks to vibration sensors, piezoelectric actuators and an appropriate instrumentation.

#### ACKNOWLEDGMENT

The research leading to these results has received funding from the European Commission under the FP7 Research Infrastructures project EuCARD, grant agreement no.227579. The authors wish to express their thanks to D. Schulte, J. Pfingstner and K. Artoos from C.E.R.N., for this project and fruitful collaboration.

#### REFERENCES

- [1] T.S. Virdee, "The LHC project: The accelerator and the experiments", Nuclear Instruments and Methods in Physics Research A, 2010, doi:10.1016/j.nima.2010.02.142.
- [2] R.W. Assmann et al., "A 3 TeV e+ e- Linear Collider Based on CLIC Technology", CERN European Organization for Nuclear Research, 28 July 2000.
- [3] N.Geffroy, L.Brunetti, B.Bolzon, A.Jeremie, B.Caron, J.Lottin "Active stabilisation studies at the sub-nanometre level for future linear colliders." Mecatronic 2008.
- [4] Brüel & Kjaer Company, controller 7537A.
- [5] B. Bolzon et al., "Etudes des vibrations et de la stabilisation à l'échelle sous-nanométrique des doublets finaux d'un collisionneur linéaire", Thesis, Annecy, 2007.
- [6] T.S. Virdee, "The LHC project: The accelerator and the experiments", Nuclear Instruments and Methods in Physics Research A, 2010, doi:10.1016/j.nima.2010.02.142.
- [7] The CMS Collaboration, "The CMS experiment at the CERN LHC", Journal of Instrumentation 3S08004 (2008) 26–89 <http://www.iop.org/EJ/journal/-page=extra.lhc/jinstS>.
- [8] B. Bolzon et al., "Linear collider test facility: ATF2 final focus active stabilization pertinence", 23rd Particle Accelerator Conference "PAC09", Vancouver : Canada , 2009.
- [9] R. Assmann et al., "Stability Considerations for Final Focus Systems of Future Linear Colliders", Proc. EPAC2000. CERN-SL-2000-059-OP. CLIC-Note-448. SLAC-REPRINT- 2000-095. DESY-M-00-04I.
- [10] J. Ellison et al., "Passive vibration control of airborne equipment using a circular steel ring", Journal of Sound and Vibration, Volume 246, Issue 1, 6 September 2001, Pages 1-28
- [11] S. Redaelli, "Stabilization of Nanometer-Size Particle Beams in the Final Focus System of the Compact Linear Collider (CLIC)", Thesis, Lausanne, 2003.
- [12] TMC Company, "TMC STATIS 2000 Stable Active Control Isolation System", Users manual, Document P/N 96-26690-02 Rev. D, November 2002.
- [13] The MathWorks, Inc.
- [14] CEDRAT Group.
- [15] Physik Instrumente (PI) GmbH & Co. KG.
- [16] I.D. Landau and G. Zito, "Digital Control Systems: Design, Identification and Implementation (Communications and Control Engineering)", January 1, 2006.
- [17] The CMS Collaboration, "The CMS experiment at the CERN LHC", Journal of Instrumentation 3S08004 (2008).